Biosensors and Bioelectronics 137 (2019) 229–235

Contents lists available at ScienceDirect

Biosensors and Bioelectronics

journal homepage: www.elsevier.com/locate/bios

Towards pharmacological treatment screening of cardiomyocyte cells using Si nanowire FETs

Ihor Zadorozhnyi, Hanna Hlukhova, Yurii Kutovyi, Volodymyr Handziuk, Nataliia Naumova, Andreas Offenhaeusser, Svetlana Vitusevich*

Bioelectronics (ICS-8), Forschungszentrum Juelich, 52425, Juelich, Germany

ARTICLE INFO

Keywords:
Bioelectronics
Nanowire
Cardiomyocytes
Action potential
Fluorescence
Lab-on-chip

ABSTRACT

Silicon nanowires (Si NWs) are the most promising candidates for recording biological signals due to improved interfacing properties with cells and the possibility of high-speed transduction of biochemical signals into detectable electrical responses. The recording of extracellular action potentials (APs) from cardiac cells is important for fundamental studies of AP propagation features reflecting cell activity and the influence of pharmacological substances on the signal. We applied a novel approach of using fabricated Si NW field-effect transistors (FETs) in combination with fluorescent marker techniques to evaluate the functional activity of cardiac cells. Extracellular AP signal recording from HL-1 cardiomyocytes was demonstrated. This method was supplemented by studies of the pharmacological effects of stimulations using noradrenaline (NorA) as a modulator of functional activity on a cellular and subcellular levels, which were also tested using fluorescent marker techniques. The role of calcium alteration and membrane potential were revealed using Fluo-4 AM and tetramethylrhodamine, methyl ester, perchlorate (TMRM) fluorescent dyes. In addition, chemical treatment with sodium dodecyl sulfate (SDS) solutions was tested. The results obtained demonstrate positive prospects for AP monitoring in different treatments for studies related to a wide range of myocardial diseases using lab-on-chip technology.

1. Introduction

Signal recordings from individual electrically active living cells (e.g., cardiomyocytes or neurons) represent the general approach for understanding biological processes in living systems on different levels, from the cellular network to the single-cell level. The heart is a particularly important system to study since it is the engine of the human body ensuring a continuous flow of blood and supplying the organism with oxygen and nutrients. Heartbeat fluctuations may be caused by a variety of factors, among which cardiac dysfunction and cardiac diseases occupy the highest priority for medical treatment and healthcare applications. Despite the current progress in developing recording electrodes for cell activity monitoring (Kaneko et al., 2018; Law et al., 2009; Santoro et al., 2013), there is still a huge requirement for devices to allow stable and reproducible in vitro evaluation of the effect of pharmacologically active agents on the tissue. Microelectrode array (MEA) chips have attracted much attention in this field and have replaced large-scale electrodes as they are capable of gaining more detailed information (Caluori et al., 2019; Timko et al., 2009) than conventional electrodes. Even though high-resolution MEAs have been developed, the signal-to-noise ratio (SNR) is still limited while electrodes are becoming smaller (Banks et al., 2002; Prohaska et al., 1986). This creates a number of challenges in terms of achieving cellular and subcellular resolution for recording functional signals.

Silicon (Si)-based devices, on the contrary, fabricated using technology compatible with modern complementary metal-oxide-semiconductor (CMOS) process, possess a lot of advantages due to their unique properties, which have been demonstrated by extensive research over the past few decades. Furthermore, a transition from conventional planar devices to nanoscaled structures such as nanowires (NWs) may improve the sensitivity down to the single molecule level. An enhanced sensitivity of biosensors based on Si NWs was confirmed for a variety of biological test objects, including proteins, nucleic acids, and viruses (Namdari et al., 2016; Zhou et al., 2017). The characteristic sizes of such structures allow much denser packaging, resulting in higher spatial resolution. It should be emphasized that recent research on interfacing between living cells and nanoscale objects demonstrates improved interface properties without cleft between a cell and

* Corresponding author.
E-mail address: s.vitusevich@fz-juelich.de (S. Vitusevich).

https://doi.org/10.1016/j.bios.2019.04.038
Received 23 February 2019; Received in revised form 11 April 2019; Accepted 16 April 2019
Available online 25 April 2019
0956-5663/

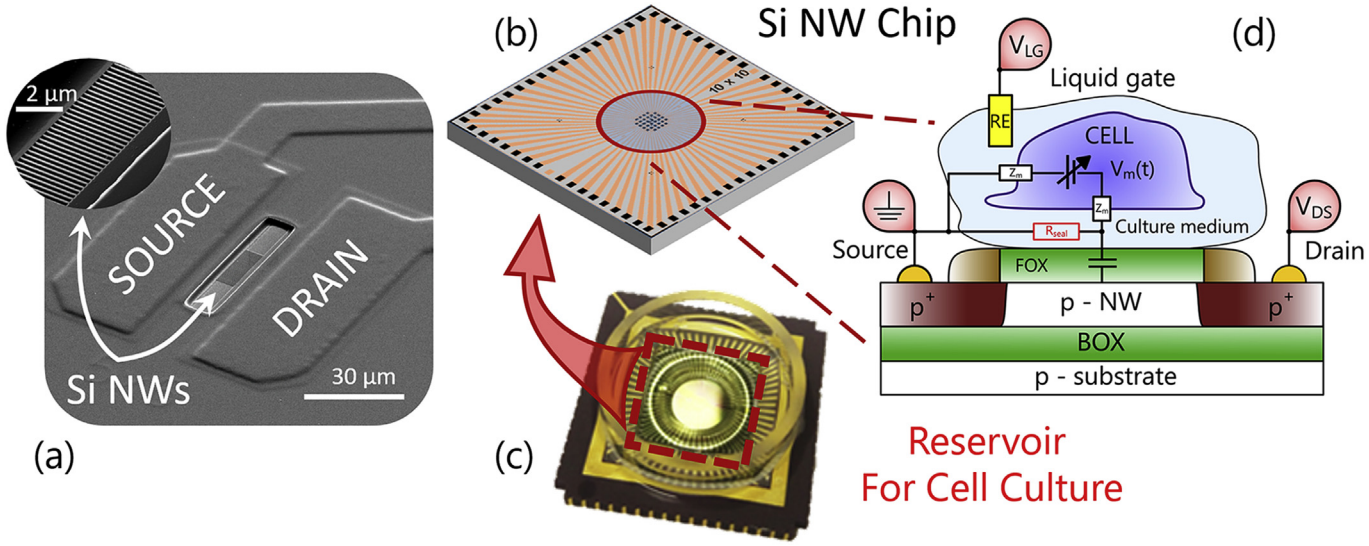

Fig. 1. (a) SEM image of a Si NW FET biosensor. The entire surface including metal feedlines is covered with polyimide passivation layer while only the active area with nanowires being exposed to the cell culture medium. Inset shows an enlarged part of the active sensing area with a nanowire array. (b) Nanowire chip with a grid layout containing 32 measurement channels. (c) Chip encapsulated within a glass ring and PDMS as a reservoir for the medium and cell culture. (d) Schematic cell-nanowire interface with the measurement configuration for cardiomyocyte electrical activity monitoring using NW FET biosensor. Typical cardiomyocytes cover the area in the range of 120–350 μm^2.

nanoscale structure in comparison to large-scale planar devices(Lee et al., 2010). Furthermore, the investigations of the gate coupling effect in nanowire transistors demonstrate the possibility of enhanced signal-to-noise ratio(SNR) for cellular recordings (Pud et al., 2014).

Modern drug design and delivery are not possible without fully understanding the drug-related metabolism and reactions as well as its ability to penetrate cells, its interaction with the target, and its pharmacological effect (Etrych et al., 2016; White and Errington, 2005). In particular, heart failure treatment requires a comprehensive and complex investigation of the functional activity of heart tissue. Dysfunction is typically caused by biochemical changes in metabolic processes on the cellular and subcellular levels. Such processes are supported by and highly interconnected with the calcium content in cells and the cellular Ca^{2+} stores in mitochondria (Bertero and Maack, 2018; Bravo-Sagua et al., 2017).

The investigation of different aspects of drug delivery and calcium transport monitoring on the cellular and subcellular levels is possible using fluorescence microscopy (Etrych et al., 2016; White and Errington, 2005). A method for a simultaneous measuring mitochondrial Ca^{2+} uptake and mitochondrial membrane potential in living cells using fluorescent dyes is described in (McKenzie et al., 2017). However, studies of noradrenaline (NorA) influence on a cell activity using this method in combination with Si NW field-effect-transistor (FET) sensors have not yet been reported.

In this work, we combine in vitro monitoring of cardiomyocyte cell culture action potential (AP) activity using Si NW FETs with fluorescence microscopy to develop a bio-platform that enables us to reveal the effect of pharmacologically active agents on the living cell community by tracking the cell calcium content, mitochondrial membrane potential, and cellular electrical spiking activity. We demonstrate the high-quality material and electrical properties of fabricated Si NW FET structures. We show that transistors operate without leakage current in culture media due to multi-stage fabrication process optimization. We apply the novel approach of using Si NW structures as a bio-platform in combination with fluorescence microscopy techniques to monitor the effects of pharmacologically active agents such as NorA on the cells' functional activity. The results of studies on the pharmacological treatment and electrical activity of HL-1 cells demonstrate that Si NW FETs can be used to investigate and select biologically active solutions to tune and control cardiac activity from the viewpoint of different physiological and pathological conditions of cardiac activity.

2. Materials and methods

2.1. Materials

SOI wafers were purchased from SOITEC. Phosphate buffered saline (10 mmol/L calcium-free PBS pH = 7.4), 5 µg/mL fibronectin, 0.2 µg/mL gelatin, Claycomb medium, 10% fetal bovine serum (FBS), penicillin-streptomycin mixture with 100 U/mL penicillin and 100 µg/mL streptomycin, 0.1 mmol/L noradrenaline (NorA), 2 mmol/L L-glutamine, and concentrated sodium dodecyl sulfate (SDS) were all purchased from Sigma-Aldrich (St. Louis, MO, USA). 10 µmol/L calcein AM and 2 µmol/L Fluo-4 AM were purchased from Life Technologies, 300 nmol/L DAPI from Thermo Fisher Scientific, and 200 nmol/L tetramethylrhodamine, methyl ester, perchlorate (TMRM) were supplied by Invitrogen. Pellet Ag/AgCl reference electrodes E−205 were purchased from Science Products.

2.2. Fabrication procedure

Si NW FETs were fabricated using a CMOS-compatible top-down approach. The fabrication process is based on silicon-on-insulator (SOI) wafers with a 70 nm thick initial active Si layer, which was thinned down to 50 nm after processing. E-beam lithography was utilized to pattern NW arrays. We used tetramethylammonium hydroxide (TMAH) wet chemical etching to transfer the NW pattern to silicon. This resulted in almost atomically flat NW surfaces. The structures used to detect extracellular APs were 20 µm in length, and each NW in the array was 150 nm in width with a spacing of 250 nm (Fig. 1). An 8 nm thick SiO_2 layer was thermally grown to serve as a gate dielectric. The source and drain contacts were highly implanted with boron ions, resulting in a p^+-p-p^+ structure. Polyimide PI-2545 was patterned using lithography and cured in order to create a stable passivation that was compatible with the cell culture. After the fabrication process, wafers were cut into chips, wire-bonded to chip carriers, and subsequently encapsulated with polydimethylsiloxane (PDMS) and glass rings to form a reservoir for the cells and the medium. Liquid-gate voltage was applied to the sample using commercially available Ag/AgCl pellet reference electrode immersed into the culture medium. Recording of cellular activity

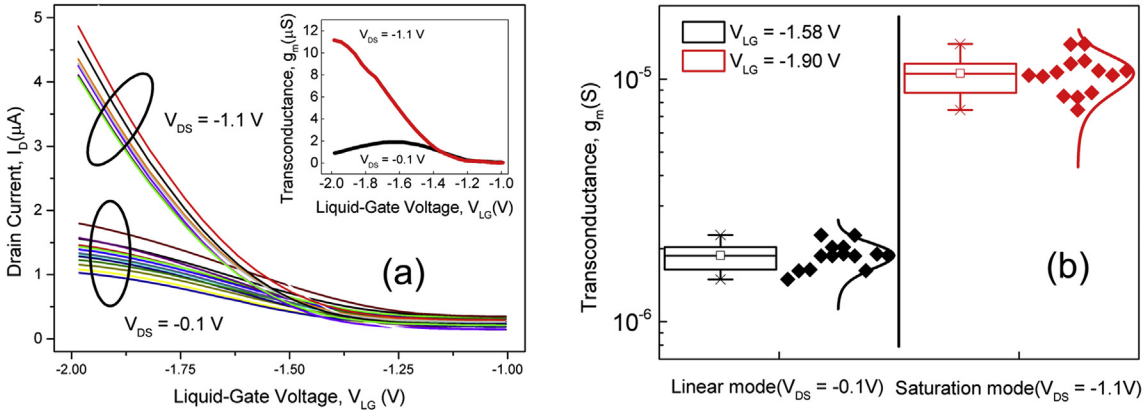

Fig. 2. (a) Transfer characteristics measured for different FETs at $V_{DS} = -0.1$ V and $V_{DS} = -1.1$ V. Inset demonstrates the transconductance averaged for all FETs; (b) The distribution of transconductance values for different FETs. Values demonstrate improved transconductance in saturation mode in comparison to linear mode, which is more favorable for cell activity monitoring.

is schematically shown in Fig. 1d.

2.3. Preparation of cardiomyocytes

In our research we used the HL-1 mouse cardiomyocyte cell line, which has been extensively used to study pathological and physiological cardiac conditions (Andersson et al., 2009; Chaudary et al., 2004; Gonnerman et al., 2012; Kuznetsov et al., 2015; Smith et al., 2012). HL-1 is an immortalized cell line that is able to continuously divide and spontaneously contract while maintaining a differentiated cardiac phenotype. HL-1 can be serially passaged without losing its differentiated cardiomyocyte phenotype, including its morphological, biochemical, and electrophysiological properties. It is well-known that HL-1 cells have been used to study normal cardiomyocyte function with regard to signaling, electrical, metabolic, and transcriptional regulations. At the same time, HL-1 cells can also be used to study pathological conditions such as hypoxia, hyperglycemia, hyperinsulinemia, apoptosis, and ischemia-reperfusion injury.

HL-1 cardiomyocyte cell line was stored and received in a frozen state. First, cells were thawed at room temperature and then passaged into T25 culture flasks for several days until the surface was fully covered. The grown cell layer demonstrated beating and electrical activity with a frequency of ~1–3 Hz (Sartiani et al., 2002).

Prior to seeding the cardiomyocytes, Si NW chips were cleaned with a 70% ethanol solution to remove any dirt from the surface. In addition, the surface of the Si NW arrays was covered with a mixture of fibronectin (5 μg/mL) dissolved in gelatin (0.2 μg/mL) for 1 h at 37 °C to improve cellular adhesion to the silicon dioxide surface.

Once the confluent layer had formed, the cardiomyocytes were split and placed inside the on-chip reservoir (approximately 150 cells/mm^2). After cell seeding, the Si NW chips were placed into the incubator at 37 °C with 5% CO_2 gas flow. Claycomb medium was supplemented with a mixture of 100 U/mL penicillin and 100 μg/mL streptomycin, as well as 10% fetal bovine serum, 0.1 mmol/L norepinephrine, and 2 mmol/L L-glutamine. The mixture has been exchanged every day during cell growth as well as 2 h before the electrical measurements.

2.4. Fluorescence imaging of cardiomyocytes

Live/dead staining of HL-1 cardiac cells on the Si NW chips was performed using a combination of calcein AM (calcein acetoxymethylester) and DAPI (4′,6-diamidino-2-phenylindole) fluorescent dyes. A green fluorescent calcein AM dye (2 μmol/L) was loaded into cells at 37 °C for a 30-min incubation period, while a blue fluorescent DAPI dye (300 nmol/L) was loaded into cells at room temperature for a 5-min incubation period. Before loading, the cell samples were washed 3 times with PBS and then incubated under appropriate conditions and concentration of the probes. After loading calcein AM and DAPI, the stain solutions were removed and the cell samples were washed with PBS 3 times for 3 min. Fluorescence imaging of HL-1 cells was performed using a ZEISS ApoTome with Axio Imager Z1 fluorescence microscope.

3. Results and discussion

3.1. Liquid-gate measurements

To measure the confluent cell layer formed on the chip, we used a multichannel measurement setup. The system enables I–V characterization to be performed as well as time-series recordings in parallel from all 32 transistors on the chip (Jansen, 2014). The setup consist of an amplification cascade which includes a pre-amplifier and a main amplifier. For AC-coupled measurements, filters were used to prevent aliasing effects. The amplified signal was then passed to the data acquisition (DAQ) system for readout and further data processing on the computer. Commercially available DAQ system converts voltage, coming from the main amplifier into 16-bit digital values. The system provides the conversion bandwidth of 1.25×10^6 samples per second. Typically 1 kHz sampling rate is used when multichannel recordings are performed. The pre-amplifier consists of a corresponding operational amplifier and a Si NW FET on the chip (the “channel”). The resulting amplification depends on the feedback resistance (R_{FB}) connected to the operational amplifier and the actual transconductance of the FET defined by the selected working point: $V_{out} = V_{LG} \times g_m \times R_{FB}$. It should be noted that for optimal signal amplification, R_{FB} corresponds approximately to the FET channel resistance.

In order to select the working point with the highest transconductance for the FETs, I–V characteristics were measured prior to the timetrace studies. The measured transfer characteristics, as shown in Fig. 2, demonstrated typical behavior for p-type transistors.

Transfer curves were measured in the linear ($V_{DS} = -0.1$ V) and saturation ($V_{DS} = -1.1$ V) regimes. The average transconductance curves for both linear and saturation regimes with an average deviation of ~12% for different FETs is shown in the inset of Fig. 2a. In the linear regime with $V_{DS} = -0.1$ V and $V_{LG} = -1.58$ V the maximum transconductance obtained was about (1.88 ± 0.23) μS for our FETs. In the other working point near the saturation regime FETs demonstrated higher transconductance values (Fig. 2b), with the maximum equal to (10.57 ± 1.91) μS at $V_{DS} = -1.1$ V and $V_{LG} = -1.9$ V. Extracted effective mobility was estimated to be around 340 cm^2/V in the linear regime. Results of studies of nanowire structures fabricated with different lengthaccording to transmission line model (TLM) confirmed that

the contribution of the contact resistance into total resistance is negligibly small.

Optimized values for drain-source, liquid-gate, and back-gate voltages were selected based on replotted derivative (dI_{DS}/dV_{LG}) curves. Further reported time series had already been recalculated into the input voltage fluctuations using the equation: $dV_G = dV_{out} / (g_m \times R_{FB})$.

A cardiomyocyte HL-1 cell community was cultured on NW FET chips. The confluent layer formed on the Si NW FETs was characterized using fluorescence microscopy visualization. The high viability of cells was assessed using calcium-sensitive fluorescent dye calcein AM and DNA-binding fluorescent dye DAPI. The electrical measurements performed demonstrate stable recordings with high SNR of recorded AP signals. The analysis of the recordings showed the propagation of APs across the cell community with a speed of ~13 mm/s, which is in good agreement with the speed values reported in the literature for cardiac cells on MEAs (Hofmann et al., 2010; Maybeck et al., 2014) and graphene FETs (Kireev et al., 2017). Analyzing signal propagation allowed us to estimate the position of pacemaker cells, which provides important information on the functional activity and communications of the entire cell community, as will be shown below.

3.2. In vitro HL-1 cell measurement

The recording of extracellular APs from cardiac cells is important for fundamental studies of AP propagation features reflecting cardiomyocyte activity as well as the influence of pharmacological substances on the signal. We applied the fabricated Si NW FETs as a bio-platform to monitor the APs and to evaluate the effects of pharmacological and electrical stimulations on the cardiac cell activity.

The cardiomyocyte cell community was cultured on the chip for 3–4 days. This time frame was sufficiently long for the cells to create a dense confluent layer that already demonstrated beating activity. High cellular vitality was confirmed by live/dead staining of the grown cells on Si NW chips using green fluorescent calcein AM dye and blue fluorescent DAPI dye (Fig. 3a). The activity within the cell culture was supported by the spontaneous generation of APs by the pacemaker cell.

Usually, pacemaker cells are the strongest and they set the beating rate for the entire monolayer, providing a stable beating rhythm for the cell community as well as the synchronization between cells (Kojima et al., 2006). Since the HL-1 cells form a syncytium, the electrical signals propagate geometrically along the tissue.

It is therefore important to record not only the electrical activity of cells but also the propagation of the signal across the community. We

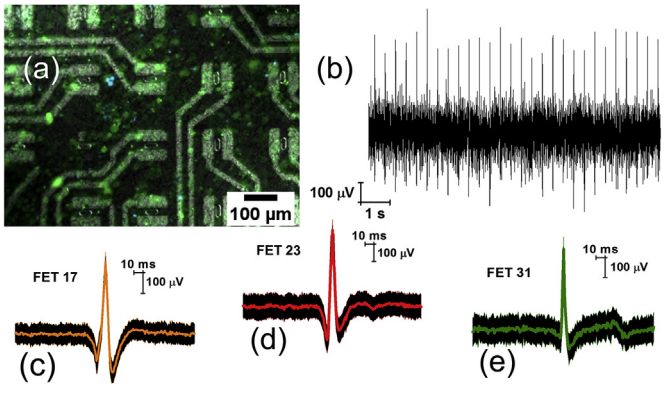

Fig. 3. (a) Live/dead staining of HL-1 cardiac cells on Si NW chips using green fluorescent calcein AM dye and blue fluorescent DAPI dye; (b) Typical recorded timetrace with action potential activity; (c),(d),(e) Extracted action potential shapes for FETs 17, 31, 23. The colored lines show averaged values for action potentials found in the timetrace, while the black background shows the standard deviation. (For interpretation of the references to color in this figure legend, the reader is referred to the Web version of this article.)

demonstrate that our NW sensors satisfy these requirements and contain multiple Si NW FETs on the chip. This enabled us to record electrical fluctuation from all 32 FETs simultaneously. Prior to time-dependent measurements, we performed I–V characterization of transistors on the chip (see data of Fig. 2).

We recorded timetraces at a sampling rate of 1 kHz with the working point set in the linear regime with $V_{DS} = -0.1$ V and $V_{LG} = -1.58$ V. The maximum transconductance obtained was about (1.88 ± 0.23) µS for our FETs. We then performed time-series measurements at another working point near the saturation regime. The FETs demonstrated higher transconductance values (Fig. 2), with the maximum equal to (10.57 ± 1.91) µS at $V_{DS} = -1.1$ V and $V_{LG} = -1.9$ V. In this working regime, clear APs were recorded with an improved 3–5 times peak-to-peak values of signal-to-noise ratio (SNR) compared to the low-voltage regime. Selection of the working regime allows to obtain enhanced SNR as it was reported previously (Pud et al., 2014). This demonstrates the advantages of using active NW FET structures compared to high-resolution MEAs. Typical recorded timetrace is shown in Fig. 3b and APs extracted for the different channels are shown in Fig. 3c, d, e. We used in-house developed software, which allows to find APs in the timetrace, extract them, align on the time axis, and average. The colored lines correspond to the mean value of multiple APs, and black background shows the standard deviation of the APs recorded over the entire measurement time.

The shape of the signal was in good agreement with the processes taking place in the cell membrane and corresponded to current flows through ion channels (Fromherz, 1999). The beating frequency was about 2–3 Hz. High peak-to-peak SNR values ranging from 3 to 5 were obtained. In general, noise may be caused by several factors (Vitusevich and Zadorozhnyi, 2017), including the quality of cell–chip coupling, sealing resistance, and junction resistance, which may also influence the transconductance of the FET itself. AP propagation across the tissue was also registered using spatially separated FETs. For the studies of signal propagation in 1D along the single line of transistors and 2D over the surface of the chip we employed linear and grid chip layouts correspondingly. In the linear configuration from measured data we recalculated the time delay of pulses for the FET channels and plotted it as a function of the transistor position in the Y direction (Fig. 4a). Time delays for seven of the transistors fitted with linear dependence, demonstrating signal propagation without distortion. Extracted AP propagation speed in the Y direction was calculated to be ~13 mm/s, which is in good agreement with the values obtained for MEA sensors (Hofmann et al., 2010; Maybeck et al., 2014) as well as for graphene field-effect transistors (Kireev et al., 2017).

As shown in Figs. 4a and 5b, one of the transistors reflected signal propagation in the opposite direction to that previously discussed. Indeed, a single pacemaker cell in the cell network caused excitation of the whole network.

We estimated the position of this pacemaker cell by plotting another line with a slope corresponding to the same propagation speed. As shown in Fig. 4a, the relevant pacemaker cell was located close to FET #23. For the propagation over the chip surface measurements were performed on the chip with grid layout (Fig. 5). In this case, transistors were distributed over the surface of the chip in 2D and we recorded spiking activity on the majority of transistors. Fig. 5a shows, that the signal also propagated over the surface of the chip with a speed of ~10 mm/s, which is also in good agreement with previous measurements. This demonstrates that we obtained high-quality signal propagation within the cellular layer, where the confluent layer was established over the entire chip sensing area.

To determine the influence of pharmacological solutions on AP and to test the biological response to the pharmacological effect on the cultured cells, we utilized noradrenalin (NorA), which is a drug used for heart stimulation and a substance that is released as a reaction to stress or danger. Cell beating depends on a direct stimulation effect caused by NorA on pumping Na^+ and K^+ cell channels. As shown in Fig. 6a, the

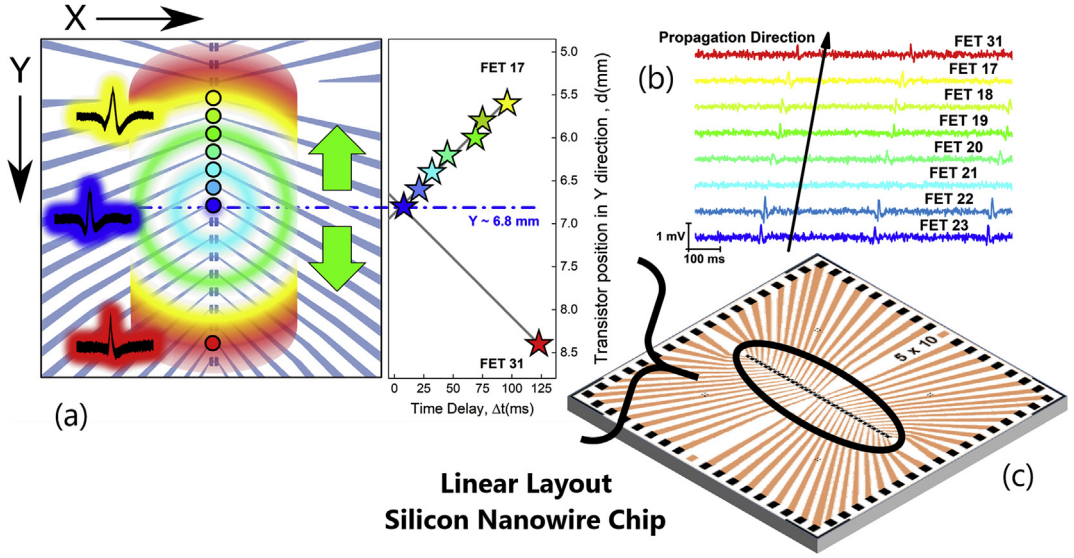

Fig. 4. (a) (left) Zoomed in nanowire chip and schematically demonstrated action potential propagation along the line of transistors. (right) The plot of action potential delay in time versus the position of the transistor which recorded the action potential. Color is used for the visual representation of the time delay. The blue line shows the approximate position of the pacemaker cell and green arrows show the directions of action potential propagation. (b) The timetraces recorded on different transistors where the action potential activity was detected. Colors correspond to the time delays in (a). Time series are sorted correspondingly to the time delay. (c) Silicon nanowire chip with the linear layout. (For interpretation of the references to color in this figure legend, the reader is referred to the Web version of this article.)

addition of NorA to the medium resulted in almost doubling the beating frequency, which is in good agreement with the literature (Natarajan et al., 2004). It should be noted that we performed a set of measurements using linear as well as grid layout chips. We demonstrate the proof of principle for cell treatment studies with noradrenaline as an example of well-established treatment of cardiac cells and changes in cell dynamic response.

Additionally, sodium dodecyl sulfate (SDS) solution was used to prove that the origin of spiking activity is referred to HL-1. Moreover, SDS may be used to model the critical stage of acute myocardial infarction (AMI) since it dissolves the cellular membrane and thus diminishes cellular activity. Supplying SDS to the medium perforates the cellular layer. These processes cause the AP activity to vanish, as it is demonstrated in Fig. 6b. Performed experiments show that Si NW FETs are the perfect candidates for studying cellular network behavior at different conditions.

3.3. Combination of electrical monitoring with fluorescent microscopy

The monitoring of AP spiking activity is not only required to evaluate cellular functional activity but also to estimate the intracellular calcium content as well as membrane potential of mitochondria. During the past two decades, calcium accumulation in mitochondria has emerged as a biological process of utmost physiological relevance. Mitochondria together with the endoplasmic and sarcoplasmic reticulum are the most important intracellular stores (Giorgi et al., 2018). Mitochondrial Ca^{2+} uptake was shown to control intracellular Ca^{2+} signaling, cell metabolism, cell survival, and other cell-type specific functions by buffering cytosolic Ca^{2+} levels and regulating mitochondrial effectors. Mitochondria are in close interconnection with the (endo) sarcoplasmic reticulum and the sites of contacts between mitochondria and the reticulum (called mitochondria-associated membranes (MAMs)) are microdomains of high Ca^{2+} concentration. In a wide range of cardiac diseases, alterations in Ca^{2+} handling, energetic deficit, and oxidative stress in cardiac myocytes are important pathophysiological hallmarks (Franzoso et al., 2016; Kim et al., 2018).

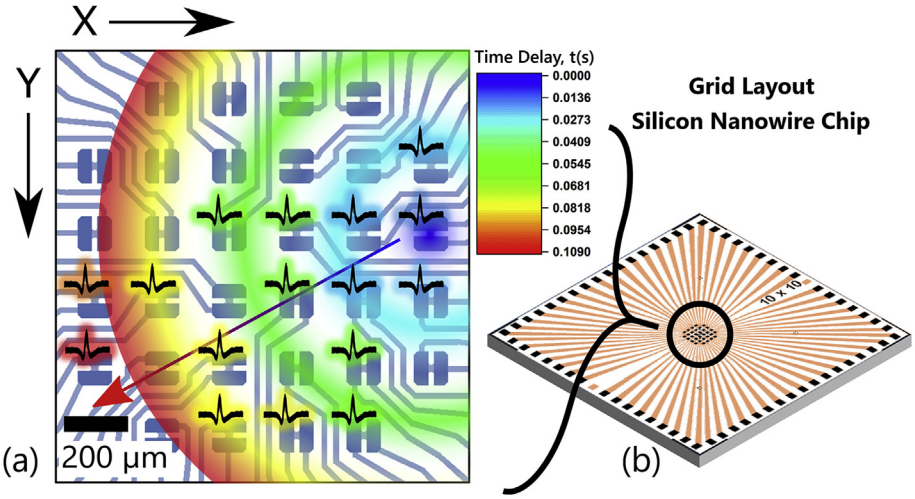

Fig. 5. (a) Zoomed in nanowire chip and schematic demonstration of action potential propagation across the surface of the chip. Action potential symbol indicates that the transistor at this position was recording action potential activity. The color indicates the time delay of the action potentials at different positions on the chip. The arrow shows the radial direction of action potential propagation (b) Silicon nanowire chip with grid layout. (For interpretation of the references to color in this figure legend, the reader is referred to the Web version of this article.)

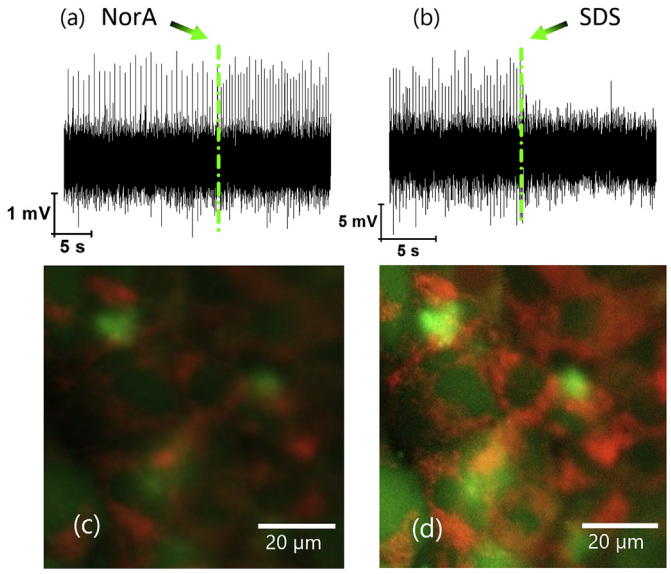

Fig. 6. (a) The influence of NorA on AP activity makes the beating rate almost twice as fast. (b) The addition of SDS results in the complete AP activity ceasing. (c) Evaluation of the functional activity of HL-1 cardiac cells on Si NW chips using green fluorescent Fluo4 AM dye and red fluorescent TMRM dye before NorA treatment. (d) The effects of NorA on the polarization of mitochondria and on the calcium level in HL-1 cells on Si NW FETs after NorA treatment. (For interpretation of the references to color in this figure legend, the reader is referred to the Web version of this article.)

Cellular functional activity studies were accomplished by applying the fluorescent markers technique. Intracellular calcium level and mitochondrial membrane potential of HL-1 cardiomyocyte cells were evaluated using a combination of Fluo-4 AM and tetramethylrhodamine, methyl ester, perchlorate (TMRM) fluorescent dyes. These fluorescent dyes were used for simultaneous fluorescence imaging of the calcium level and mitochondrial membrane potential of the HL-1 cells. Green fluorescent Fluo-4 AM dye (10 µmol/L) was loaded into cells at 37 °C for a 30-min incubation period and red fluorescent TMRM dye (200 nmol/L) was loaded into cells at room temperature for a 5-min incubation period. Before loading, the cell samples were washed 3 times with PBS and then incubated under appropriate conditions and concentration of the probes. After loading with Fluo-4 AM and TMRM, the stain solutions were removed, and the cell samples were washed with PBS 3 times for 3 min.

We used a combination of calcium-sensitive Fluo-4 AM and membrane potential-sensitive TMRM fluorescent dyes to evaluate the effect of NorA on the functional activity of HL-1 cardiac cells on Si NW chips. The results obtained are shown in Fig. 6c–d. Cardiac cell functional activity depends on metabolic biochemical changes on the cellular and subcellular levels and is closely connected with both the calcium content of cells and calcium stores in cells, particularly in mitochondria.

Calcium is an important secondary messenger in cardiac function (Freichel et al., 2017). Mitochondria in cardiac cells play the central role since they are the main source of adenosine triphosphate (ATP) and reactive oxygen species. Their function is critically controlled by Ca^{2+} and the polarization of the mitochondrial membrane potential (Bertero and Maack, 2018). The resting concentration of Ca^{2+} in the cytoplasm is in the range of 10–100 nmol/L. To maintain this low concentration, Ca^{2+} is pumped from the cytosol to the extracellular space and into the subcellular calcium stores of mitochondria. Signaling occurs when the cell is stimulated to release Ca^{2+} from intracellular stores, and/or when Ca^{2+} penetrates the cell through ion channels of the plasma membrane. Specific signals and stimulations can trigger an increase in the cytoplasmic Ca^{2+} level, leading to the change of mitochondrial membrane potential(Bagur and Hajnóczky, 2017). In a view of the abovementioned, the monitoring of cardiac cell activity has to be coupled with the study of the functional activity of cells and the evaluation of the Ca^{2+} content as well as membrane potential of cardiomyocytes and cardiac mitochondria (Tribulova et al., 2016).

The functional activity of HL-1 cardiac cells on Si NW chips and the effect of NorA on this activity were studied using a combination of Fluo-4 AM and TMRM fluorescent dyes.

Fluo-4 AM is a membrane-permeant AM ester form of Fluo-4 that can penetrate inside cells via incubation. It does not bind extracellular calcium, but it is readily hydrolyzed to Fluo-4 by endogenous esterases once the dye is inside the cells. Fluo-4 AM ester is very useful for measuring and visualizing the intracellular calcium level in high-throughput drug screening. It is optimally excited at the 494 nm wavelength of light and emits effectively at 506 nm.

TMRM is a membrane potential-sensitive cell-permeant dye which accumulates in active mitochondria with intact membrane potentials. It can be used to measure the membrane potential of mitochondria in living cells. TMRM does not form aggregates in cell membranes and interacts minimally with membrane proteins. Thus, the transmembrane distribution of the dye is directly related to the membrane potential (Farkas et al., 1989; Gerencser et al., 2012).

We applied the combination of calcium-sensitive Fluo-4 AM and membrane potential-sensitive TMRM fluorescent dyes to evaluate the functional activity of HL-1 cardiac cells on Si NW chips. The green fluorescence of Fluo-4 AM represents the level of calcium in HL-1 cells, while the red fluorescence of TMRM represents the membrane potential of mitochondria in HL-1 cells (Fig. 6c). It was shown that the HL-1 cells, cultured on the sensing surface of the Si NW FETs, were functionally active. This was confirmed by the polarization of the mitochondrial membrane (TMRM red fluorescence) as well as by the calcium content (Fluo-4 AM green fluorescence) in cells. The results are in good agreement with those reported in the literature (McKenzie et al., 2017).

Moreover, in further experiments, we used this combination of calcium-sensitive Fluo-4 AM and membrane potential-sensitive TMRM fluorescent dyes to evaluate the effect of NorA on the functional activity of HL-1 cardiac cells on Si NW chips. These experiments showed that the addition of NorA led to changes in both the mitochondrial membrane potential and the calcium level in the cells (Fig. 6d). Therefore, the effects of NorA on the polarization of mitochondria were clearly registered as increased fluorescence response, and visualized by the green fluorescent Fluo-4 AM dye and red fluorescent TMRM dye. Our results confirm the crucial role of calcium content in the functionality of cardiomyocytes with regard to the biochemical influence of NorA as an effector of heart stimulation and as a substance biomarker of stress reactions in cells. As proof that spiking activity corresponds to the cellular activity, we used SDS, which dissolves the cell membrane and can be used to model critical stages of acute myocardial infarction (AMI). Adding SDS to the medium resulted in the cellular layer being perforated and thus suppressed cellular activity, causing AP activity to cease completely. Performed studies showed that Si NW FETs are perfect candidates for the investigation of cellular network behavior under different conditions. Furthermore, in combination with calcium-sensitive fluorescent markers, they represent a novel approach for studies of cellular response to a variety of pharmacological treatments. Such experimental tools are particularly relevant for monitoring the states and stages of cardiac diseases including AMI.

4. Conclusions

We designed and developed a bio-platform based on Si NW FETs, which enabled us to monitor cellular AP spiking activity of HL-1 cells. In order to evaluate the functional activity of cardiomyocyte cells, the fluorescent imaging and electrical measurements were performed before as well as after pharmacological treatments. This novel approach opens up prospects with regard to evaluating the effect of pharmacologically active agents on cardiac tissue. Fabricated structures

demonstrated stable and high-quality FET behavior with a sufficiently high transconductance to record APs of HL-1 cells in a culture medium. Sensing devices were used for in vitro electrical activity monitoring of the cardiomyocyte cell community, which was cultured directly in a reservoir on the chip. The high SNR values of 3–5 were demonstrated for the fabricated FETs. AP propagation across the cell layer was reliably recorded. Spatially separated FETs made it possible to extract the position of pacemaker cells, which is important for studies of HL-1 cell communication and their responses to external treatments. High-quality confluent layers of cardiomyocytes were grown on Si NW chips with high cell viability and vitality, which was confirmed by fluorescence imaging with calcein AM and DAPI fluorescent markers. We studied the functional activity of the HL-1 cells on the Si NW FET platforms and demonstrated the pharmacological and biochemical effects of NorA by tracking changes in AP frequency and using Fluo-4 AM and TMRM fluorescent dyes. The increased fluorescence response was revealed after adding NorA, which is a biochemical stimulator of cell activity. The spiking activity of the cardiomyocytes ceased after the addition of SDS solution. Performed experiments show that Si NW FETs are promising candidates as a tool for the studies of cellular responses to a variety of pharmacological influences.

The results demonstrate the prospects of using the fabricated Si NW FETs as a bio-platform for studying HL-1 cells as well as to monitor cellular functional activity based on the analysis of the biochemical and electrophysiological properties of the cells. The results obtained represent a new approach for the investigation of various diseases, including myocardial dysfunctions.

Declaration of interests

The authors declare that they have no known competing financial interests or personal relationships that could have appeared to influence the work reported in this paper.

CRediT authorship contribution statement

Ihor Zadorozhnyi: Writing - original draft, Investigation. **Hanna Hlukhova:** Investigation. **Yurii Kutovyi:** Formal analysis. **Volodymyr Handziuk:** Formal analysis. **Nataliia Naumova:** Investigation. **Andreas Offenhaeusser:** Supervision. **Svetlana Vitusevich:** Conceptualization, Supervision.

Acknowledgment

Silicon nanowire devices were fabricated using the Helmholtz Nano Facility (HNF) at Forschungszentrum Juelich. Y. K. greatly appreciates a research grant from the German Academic Exchange Service (DAAD).

References

Andersson, K.B., Birkeland, J.A.K., Finsen, A.V., Louch, W.E., Sjaastad, I., Wang, Y., Chen, J., Molkentin, J.D., Chien, K.R., Sejersted, O.M., Christensen, G., 2009. J. Mol. Cell. Cardiol. 47, 180–187.
Bagur, R., Hajnóczky, G., 2017. Mol. Cell 66, 780–788.
Banks, D.J., Balachandran, W., Richards, P.R., Ewins, D., 2002. Physiol. Meas. 23, 437–448.
Bertero, E., Maack, C., 2018. Circ. Res. 122, 1460–1478.
Bravo-Sagua, R., Parra, V., López-Crisosto, C., Díaz, P., Quest, A.F.G., Lavandero, S., 2017. Comp. Physiol. 7, 623–634.
Caluori, G., Pribyl, J., Pesl, M., Jelinkova, S., Rotrekl, V., Skladal, P., Raiteri, R., 2019. Biosens. Bioelectron. 124–125, 129–135.
Chaudary, N., Naydenova, Z., Shuralyova, I., Coe, I.R., 2004. Cardiovasc. Res. 61, 780–788.
Etrych, T., Lucas, H., Janoušková, O., Chytil, P., Mueller, T., Mäder, K., 2016. J. Control. Release 226, 168–181.
Farkas, D.L., Wei, M., Febbroriello, P., Carson, J.H., Loew, L.M., 1989. Biophys. J. 6, 1053–1069.
Franzoso, M., Zaglia, T., Mongillo, M., 2016. Biochim. Biophys. Acta Mol. Cell Res. 1863, 1904–1915.
Freichel, M., Berlin, M., Schürger, A., Mathar, I., Bacmeister, L., Medert, R., Frede, W., Marx, A., Segin, S., E. Camacho Londoño, J., 2017. TRP channels in the heart. In: Emir, T.L.R. (Ed.), Neurobiology of TRP Channels, second ed. CRC Press/Taylor & Francis, Boca Raton (FL), pp. 149–186.
Fromherz, P., 1999. Eur. Biophys. J. 28, 254–258.
Gerencser, A.A., Chinopoulos, C., Birket, M.J., Jastroch, M., Vitelli, C., Nicholls, D.G., Brand, M.D., 2012. J. Physiol. 590, 2845–2871.
Giorgi, C., Marchi, S., Pinton, P., 2018. Nat. Rev. Mol. Cell Biol. 19, 713–730.
Gonnerman, E.A., Kelkhoff, D.O., McGregor, L.M., Harley, B.A.C., 2012. Biomaterials 33, 8812–8821.
Hofmann, B., Maybeck, V., Eick, S., Meffert, S., Ingebrandt, S., Wood, P., Bamberg, E., Offenhäusser, A., 2010. Lab Chip 10, 2588–2596.
Jansen, M., 2014. Schluesseltechnologien/Key Technologies.Band 82, vol. 82. Forschungszentrum Juelich, Juelich, 9783893369447pp. 181 PhD Thesis. (in German).
Kaneko, T., Toriumi, H., Shimada, J., Nomura, F., 2018. Jpn. J. Appl. Phys. 57, 1–4 03EB03.
Kim, J.C., Son, M.J., Woo, S.H., 2018. Arch. Biochem. Biophys. 659, 33–41.
Kireev, D., Zadorozhnyi, I., Qiu, T., Sarik, D., Brings, F., Wu, T., Seyock, S., Maybeck, V., Lottner, M., Blaschke, B., Garrido, J., Xie, X., Vitusevich, S., Wolfrum, B., Offenhausser, A., 2017. IEEE Trans. Nanotechnol. 16, 140–147.
Kojima, K., Kaneko, T., Yasuda, K., 2006. Biochem. Biophys. Res. Commun. 351, 209–215.
Kuznetsov, A.V., Javadov, S., Sickinger, S., Frotschnig, S., Grimm, M., 2015. Biochim. Biophys. Acta Mol. Cell Res. 1853, 276–284.
Law, J.K.Y., Yeung, C.K., Hofmann, B., Ingebrandt, S., Rudd, J.A., Offenhäusser, A., Chan, M., 2009. Physiol. Meas. 30, 155–167.
Lee, K.Y., Shim, S., Kim, I.S., Oh, H., Kim, S., Ahn, J.P., Park, S.H., Rhim, H., Choi, H.J., 2010. Nanoscale Res. Lett. 5, 410–415.
Maybeck, V., Edgington, R., Bongrain, A., Welch, J.O., Scorsone, E., Bergonzo, P., Jackman, R.B., Offenhäusser, A., 2014. Adv. Healthc. Mater. 3, 283–289.
McKenzie, M., Lim, S.C., Duchen, M.R., 2017. JoVE 119, 1–6 e55166.
Namdari, P., Daraee, H., Eatemadi, A., 2016. Nanoscale Res. Lett. 11, 1–16 406.
Natarajan, A.R., Rong, Q., Katchman, A.N., Ebert, S.N., 2004. Pediatr. Res. 56, 411–417.
Prohaska, O.J., Olcaytug, F., Pfundner, P., Dragaun, H., 1986. IEEE Trans. Biomed. Eng. BME- 33, 223–229.
Pud, S., Li, J., Sibiliev, V., Petrychuk, M., Kovalenko, V., Offenhäusser, A., Vitusevich, S., 2014. Nano Lett. 14, 578–584.
Santoro, F., Schnitker, J., Panaitov, G., Offenhäusser, A., 2013. Nano Lett. 13, 5379–5384.
Sartiani, L., Bochet, P., Cerbai, E., Mugelli, A., Fischmeister, R., 2002. J. Physiol. 545, 81–92.
Smith, A.W., Segar, C.E., Nguyen, P.K., MacEwan, M.R., Efimov, I.R., Elbert, D.L., 2012. Acta Biomater. 8, 31–40.
Timko, B.P., Cohen-Karni, T., Yu, G., Qing, Q., Tian, B., Lieber, C.M., Timko, Brian P., Cohen-Karni, Tzahi, Yu, Guihua, Qing, Quan, Tian, Bozhi, Lieber, C.M., Timko, B.P., Cohen-Karni, T., Yu, G., Qing, Q., Tian, B., Lieber, C.M., 2009. Nano Lett. 9, 914–918.
Tribulova, N., Knezl, V., Szeiffova Bacova, B., Egan Benova, T., Viczenczova, C., Gonçalvesova, E., Slezak, J., 2016. Physiol. Res. 65, S139–S148.
Vitusevich, S., Zadorozhnyi, I., 2017. Semicond. Sci. Technol. 32, 1–21 043002.
White, N.S., Errington, R.J., 2005. Adv. Drug Deliv. Rev. 57, 17–42.
Zhou, W., Dai, X., Lieber, C.M., 2017. Rep. Prog. Phys. 80, 1–29 016701.